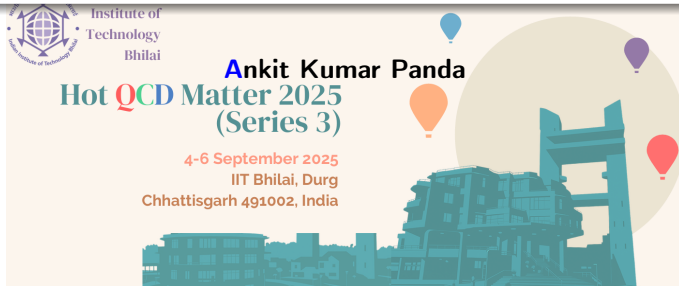


Magnetic Field Effects on Dilepton Spectra and Anisotropic Flow: A Hydrodynamical Study



Institute of
Technology
Bhilai

Ankit Kumar Panda

**Hot QCD Matter 2025
(Series 3)**

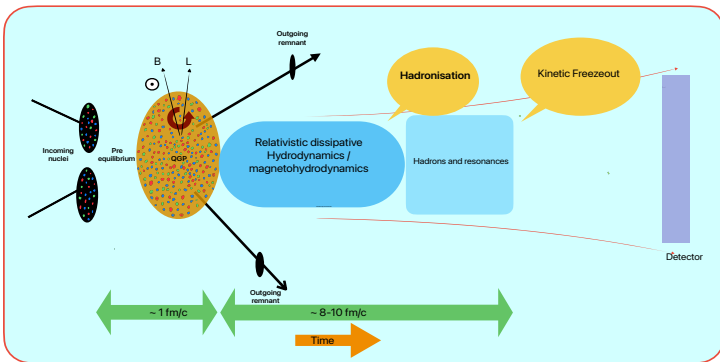
4-6 September 2025
IIT Bhilai, Durg
Chhattisgarh 491002, India

Collaborators: Dr. **Aritra Das**, Dr. **Ashutosh Dash**, Dr. **Aritra Bandyopadhyay**, Dr. **Chowdhury Aminul Islam**

Table of Contents

- 1 Heavy Ion Collisions and Magnetic Field
- 2 Why dileptons ?
- 3 Recent studies
- 4 Steps undertaken
- 5 Results

Heavy Ion Collisions and Magnetic Field



Phys. Rev. C 102, 014909 ,Phys.Lett.B 696 (2011) 328-337

- Formation of the almost **perfect fluid** (lowest $\frac{\eta}{s}$ value) (PhysRevLett.109.139904).
- Strongest Magnetic field produced in the universe of the order of $10^{18} - 10^{19}$ **Gauss** (Phys.Rev.C 89 (2014) 5, 054905).

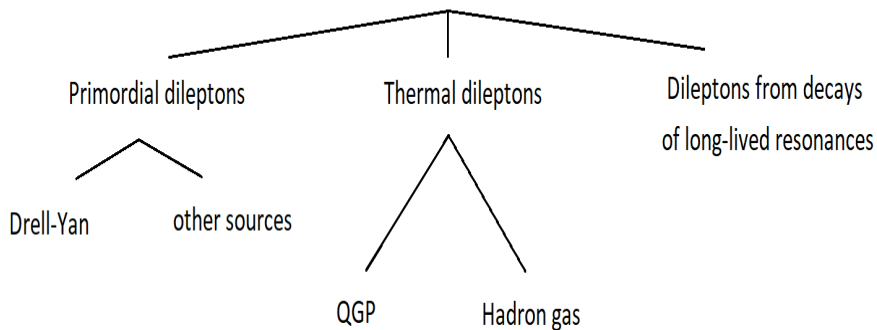
Effect of EM Fields on **Dileptons** as a Probe of the Medium

Why Study Dileptons?

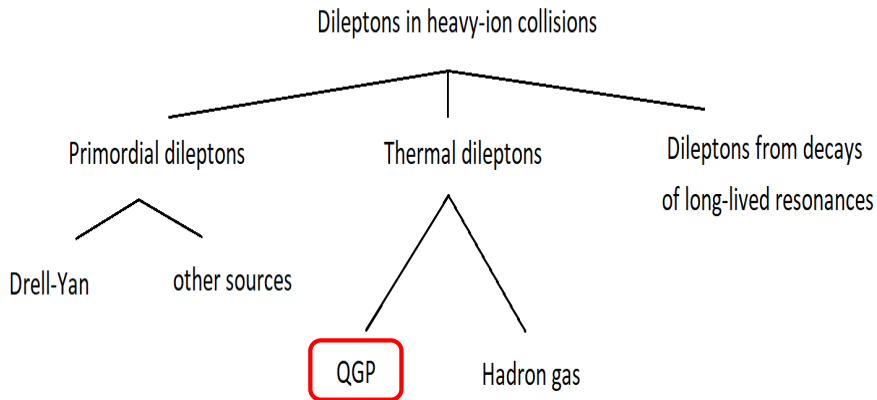
- **Dileptons** (e^+e^- , $\mu^+\mu^-$) are produced during **all stages** of a heavy-ion collision.
- Once produced, they interact only **electromagnetically** \Rightarrow **escape the medium almost unaffected**.
- \Rightarrow Act as **penetrating probes** of the hot and dense QCD matter, especially the QGP.
- **What they reveal:**
 - **Temperature** of the medium (via thermal rates),
 - **Lifetime** of the QGP,
 - **In-medium modifications** of vector mesons.

Dilepton Production Sources

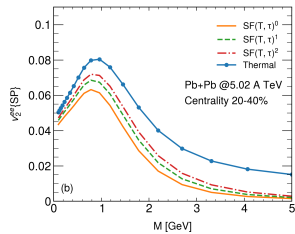
Dileptons in heavy-ion collisions



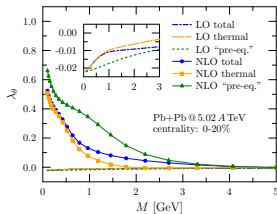
Dilepton Production Sources



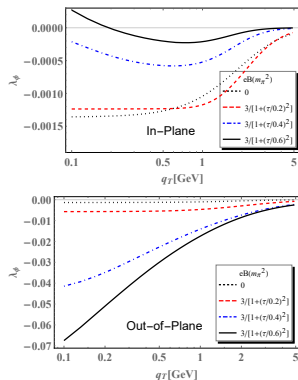
Recent Studies Using Dileptons



Xiang-Yu Wu *et al.*,
arXiv:2504.21698
Hybrid model study of pre-equilibrium
and thermal dilepton v_2 .



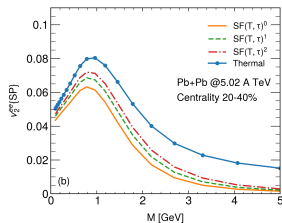
Xiang-Yu Wu *et al.*, *Hydrodynamic
evolution and dilepton polarization.*



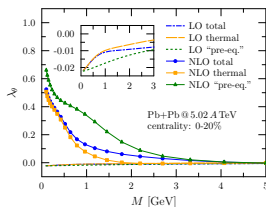
Minghua Wei & Li Yan, *Phys. Rev.
D* 110, 054024 (2024)
Magnetic field effect's study of λ_ϕ
and $\lambda_{\theta\phi}$ vs q_T .

and So on..

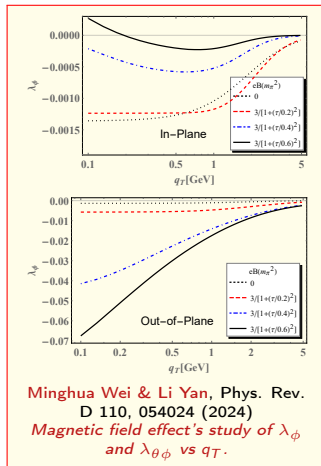
Recent Studies Using Dileptons



Xiang-Yu Wu et al.,
arXiv:2504.21698
Hybrid model study of
pre-equilibrium and thermal
dilepton v_2 .



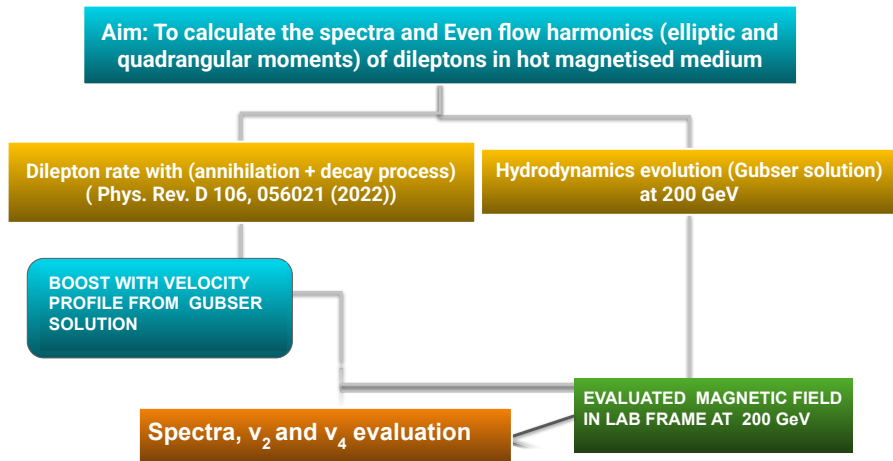
Xiang-Yu Wu et al., *Hydrodynamic
evolution and dilepton polarization.*



Minghua Wei & Li Yan, Phys. Rev.
D 110, 054024 (2024)
*Magnetic field effect's study of λ_ϕ
and λ_θ vs q_T .*

and So on.. See talk of Mr. Ashutosh for some new results on dileptons..

How did we proceed ?



Processes involved in the study of Dileptons

$$\left. \frac{dN}{d^4x d^4P} \right|_{\text{total}} = \left. \frac{dN}{d^4x d^4P} \right|_{q+\bar{q} \rightarrow \gamma^*} + \left. \frac{dN}{d^4x d^4P} \right|_{q \rightarrow q+\gamma^*} + \left. \frac{dN}{d^4x d^4P} \right|_{\bar{q} \rightarrow \bar{q}+\gamma^*} \quad (1)$$

Dilepton Production Channels in Magnetic Field:

1. Annihilation Process: $q + \bar{q} \rightarrow \gamma^*$

$$\begin{aligned} \left. \frac{dN}{d^4x M dM p_T dp_T dy d\phi_p} \right|_{q+\bar{q} \rightarrow \gamma^*} &= \frac{\alpha_{\text{EM}}^2}{3\pi^3} \frac{4N_c}{M^2} \frac{1}{e^{\frac{M_T \cosh y}{T}} - 1} \sum_{f=u,d} \left(\frac{q_f}{e}\right)^2 \sum_{\ell,n=0}^{\infty} (-1)^{\ell+n} \mathcal{N}_{\ell,n}(p_{\parallel}^2, p_{\perp}^2) \\ &\times \frac{\Theta(p_{\parallel}^2 - (m_{f,\ell} + m_{f,n})^2)}{\lambda^{1/2}(p_{\parallel}^2, m_{f,\ell}^2, m_{f,n}^2)} \\ &\times \left[2 - \tilde{n}_+(\mathcal{E}_{f,\ell,k}^+) - \tilde{n}_-(\mathcal{E}_{f,n,q}^+) - \tilde{n}_+(\mathcal{E}_{f,\ell,k}^-) - \tilde{n}_-(\mathcal{E}_{f,n,q}^-) \right] \end{aligned} \quad (2)$$

Processes involved in the study of Dileptons..

$$m_{f,\ell} = \sqrt{2\ell|q_f B| + m_f^2}, \quad n \leq \ell + \left\lfloor \frac{p_{||}^2 - 2m_{f,\ell} \sqrt{p_{||}^2}}{2|q_f B|} \right\rfloor, \quad \ell \leq \left\lfloor \frac{p_{||}^2 - 2m_f \sqrt{p_{||}^2}}{2|q_f B|} \right\rfloor$$

2. Particle Decay: $q \rightarrow q + \gamma^*$

$$\begin{aligned} \frac{dN}{d^4x M dM p_T dp_T dy d\phi_p} \Big|_{q \rightarrow q + \gamma^*} &= \frac{\alpha_{\text{EM}}^2}{3\pi^3} \frac{4N_c}{M^2} \frac{1}{e^{\frac{M_T \cosh y}{T}} - 1} \sum_{f=u,d} \left(\frac{q_f}{e}\right)^2 \sum_{\ell > n}^{\infty} (-1)^{\ell+n} \mathcal{N}_{f,\ell,n}(p_{||}^2, p_{\perp}^2) \\ &\times \frac{\Theta((m_{f,\ell} - m_{f,n})^2 - p_{||}^2)}{\lambda^{1/2}(p_{||}^2, m_{f,\ell}^2, m_{f,n}^2)} \\ &\times \left[\tilde{n}_+(\mathcal{E}_{f,\ell,k}^+) - \tilde{n}_+(-\mathcal{E}_{f,n,q}^+) + \tilde{n}_+(\mathcal{E}_{f,\ell,k}^-) - \tilde{n}_+(-\mathcal{E}_{f,n,q}^-) \right] \quad (3) \end{aligned}$$

$$\ell > n, \quad n \leq \ell + \left\lfloor \frac{p_{||}^2 - 2m_{f,\ell} \sqrt{p_{||}^2}}{2|q_f B|} \right\rfloor, \quad \ell \geq \left\lfloor \frac{p_{||}^2 + 2m_f \sqrt{p_{||}^2}}{2|q_f B|} \right\rfloor$$

Similarly for \bar{q} also...

Phys. Rev. D 106, 056021 (2022)

Important assumption:

Numerical stability in dilepton rates:

- Rates involve Laguerre polynomials $L_\ell^\alpha(\xi)$, with $\xi = p_\perp^2 / (2|q_f B|)$.
- For weak B , large ξ causes unstable evaluations.
- Introduce cutoff on ξ :

$$M = \{0.1, 0.3, 0.5\} \text{ GeV} \Rightarrow [\xi_{\text{cf}}] = \{120, 100, 50\}.$$

- Restrict Landau sums to $|eB| > 0.003 \text{ GeV}^2$.

If conditions are not satisfied:

{ Use Born rate for annihilation,
 { Set decay rates to zero.

Interested in thermal medium \Rightarrow Cutoff does not harm our purpose

Gubser flow

Fluid velocity is defined:

$$\begin{aligned} u^\tau &= \cosh \kappa \\ u^\perp &= \sinh \kappa \\ u^\eta &= 0 \end{aligned} \tag{4}$$

where

$$\kappa(x_\perp, \tau) = \text{Arctanh} \left(\frac{2q^2 \tau x_\perp}{1 + q^2 \tau^2 + q^2 x_\perp^2} \right). \tag{5}$$

$$e = \hat{e}_0 \left(\frac{4q^2}{\tau} \right)^{4/3} \left[1 + 2q^2 (\tau^2 + x_\perp^2) + q^4 (\tau^2 - x_\perp^2)^2 \right]^{-4/3}. \tag{6}$$

Gubser flow..

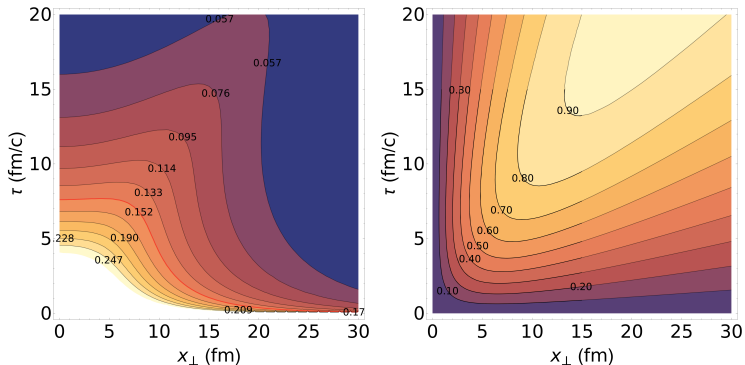


Figure: **Left panel:** Isothermal contours in the (x_{\perp}, τ) plane from Gubser's hydrodynamic solution with $\hat{T}_0 = 10.8$ and $q^{-1} = 6.4$ fm. The red curve ($T_{\min} = 0.15$ GeV) marks the freeze-out surface. **Right panel:** Contours of transverse velocity $v^{\perp}(x_{\perp}, \tau) = u^{\perp}/u^{\tau}$.

Evolution of temperature

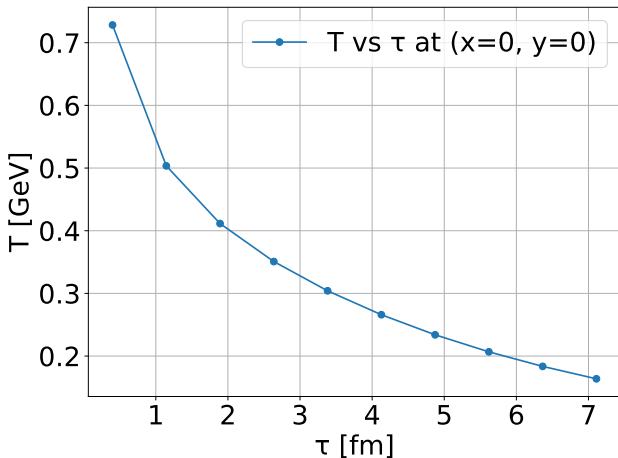


Figure: Temperature evolution with proper time at the center of the collision zone $(X, Y) = (0, 0)$ for Au+Au collisions.

Magnetic field profile

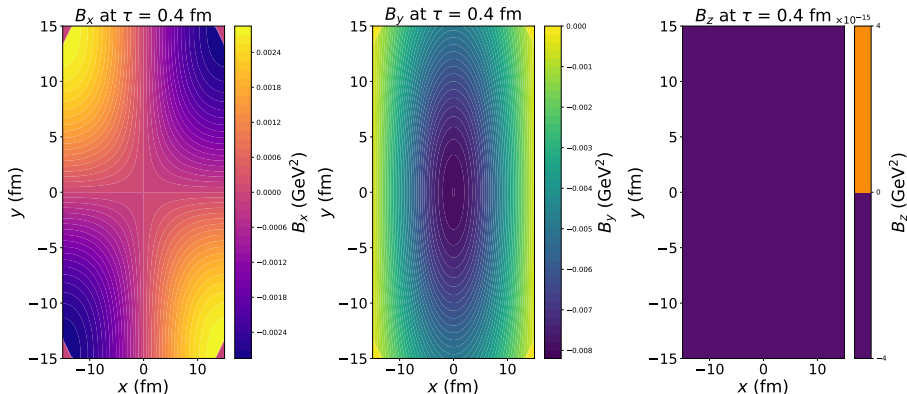


Figure: Transverse profiles of different components of the magnetic field for Au+Au collisions at $\sqrt{s_{NN}} = 200$ GeV with impact parameter $b = 12$ fm, evaluated at proper time $\tau = 0.4$ fm and electrical conductivity $\sigma = 0.58$ MeV.

Magnetic field profile

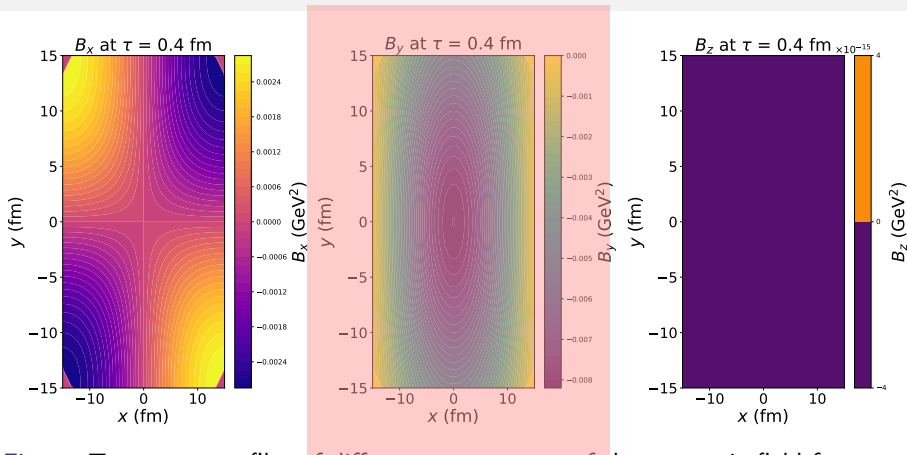


Figure: Transverse profiles of different components of the magnetic field for Au+Au collisions at $\sqrt{s_{NN}} = 200$ GeV with impact parameter $b = 12$ fm, evaluated at proper time $\tau = 0.4$ fm and electrical conductivity $\sigma = 0.58$ MeV.

The effect of the strength of the magnetic field (Spectra)

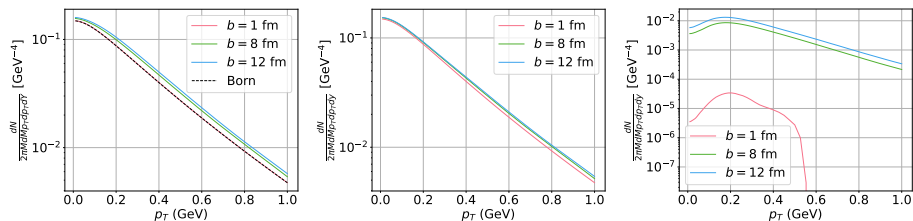


Figure: $dN/(2\pi MdMp_T dp_T dY)$ for various impact parameters at fixed $(M, \sigma, Y) = (0.1 \text{ GeV}, 5.8 \text{ MeV}, 0)$, showing the total (left) and the contribution of annihilation (middle) and decay (right) processes.

- Total spectra is dominated by the annihilation process.
- Increasing the impact parameter increases the spectra.

The effect of the lifetime of the magnetic field

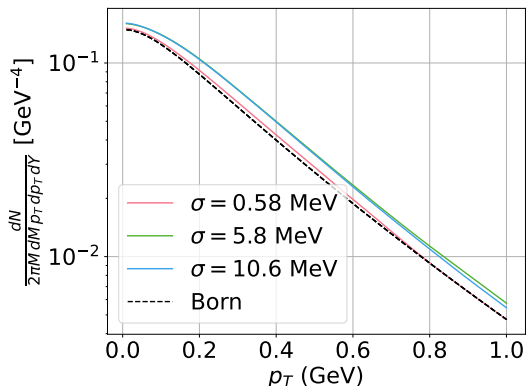


Figure: Total $dN/(2\pi M dM p_T dp_T dY)$ for different electrical conductivities at given $(M, b, Y) = (0.1 \text{ GeV}, 12 \text{ fm}, 0)$.

- Increasing the life time of magnetic field increases the spectra.

The effect of the invariant mass

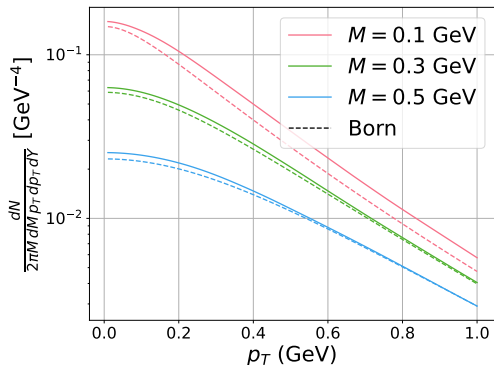


Figure: Total $dN/(2\pi M dM p_T dp_T dY)$ vs p_T at $b = 12$ fm, $\sigma = 5.8$ MeV, $Y = 0$.

- Low mass enhancement is seen in spectra.

Even-flow harmonics- v_2

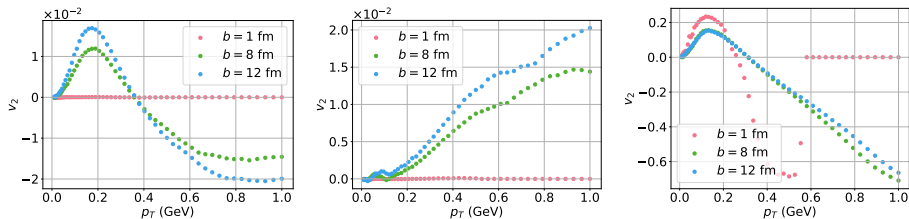


Figure: v_2 vs p_T at $(M, \sigma, Y) = (0.1 \text{ GeV}, 5.8 \text{ MeV}, 0)$. The left panel shows the total v_2 , annihilation (middle) and decay processes (right).

- v_2 is positive at low p_T but becomes negative at high p_T .
- Zero crossing is not prominent with increasing magnetic field strengths.

conti..

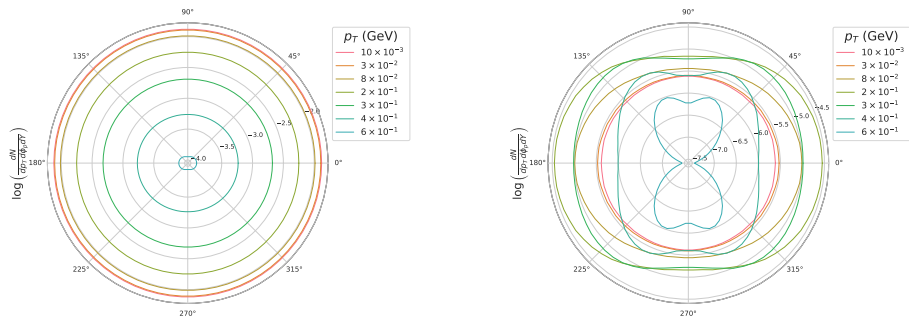


Figure: Polar plot of $\log (dN/(dp_T d\phi_p dY))$ at $(\sigma, b, Y) = (5.8 \text{ MeV}, 8 \text{ fm}, 0)$ and $M = 0.1 \text{ GeV}$, for annihilation (left) and decay (right) processes respectively.

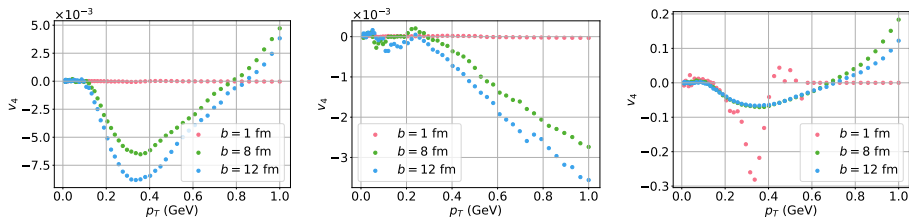
V_4 

Figure: v_4 vs p_T at $(M, \sigma, Y) = (0.1 \text{ GeV}, 5.8 \text{ MeV}, 0)$. The left panel shows the total v_4 , annihilation (middle) and decay (right) processes.

- v_4 is negative at low p_T but becomes positive at high p_T .
- Zero crossing is prominent with increasing magnetic field strengths as compared to v_2 .

Effect of lifetime of magnetic field (v_2 and v_4)

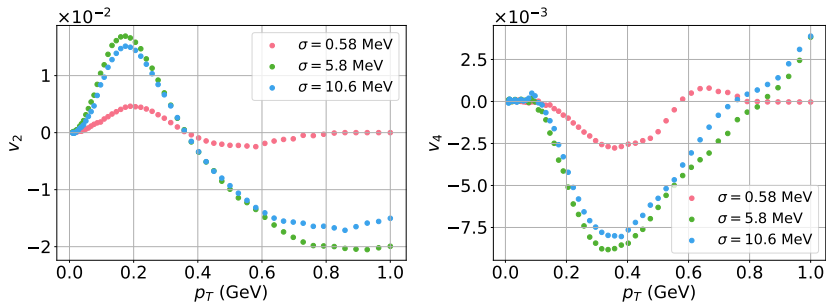


Figure: The total v_2 (left) and v_4 (right) for various electrical conductivities at given $(M, b, Y) = (0.1 \text{ GeV}, 12 \text{ fm}, 0)$, illustrating the effect of the changing medium response.

- Increasing the conductivity increases the v_2 and v_4 .
- The trend however is opposite.

Effect of Invariant mass (v_2 and v_4)

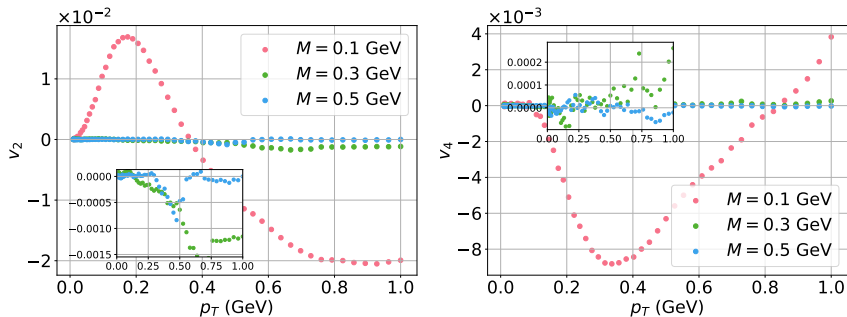


Figure: Total v_2 (left) and v_4 (right) for various invariant masses at fixed $(b, \sigma, Y) = (12 \text{ fm}, 5.8 \text{ MeV}, 0)$.

- Enhancement at low mass is clearly visible.

Summary of Results

- Both the spectra and flow coefficients (v_2 , v_4) **increase** with larger impact parameter and higher conductivity.
- v_2 is **positive** at low p_T and turns **negative** at higher p_T , whereas v_4 shows the opposite trend.
- While annihilation dominates, decay processes also contribute significantly and provide a clear signature of magnetic fields, with non-zero v_2 and v_4 even in nearly central collisions.
- The spectra show a strong **enhancement** at low invariant masses, which gradually **diminishes** at higher p_T .
- For v_2 and v_4 , distinct differences are observed at low invariant mass (around 0.1 GeV) compared to higher mass regions.

Summary of Results

- Both the spectra and flow coefficients (v_2 , v_4) **increase** with larger impact parameter and higher conductivity.
- v_2 is **positive** at low p_T and turns **negative** at higher p_T , whereas v_4 shows the opposite trend.
- **While annihilation dominates, decay processes also contribute significantly and provide a clear signature of magnetic fields, with non-zero v_2 and v_4 even in nearly central collisions.**
- The spectra show a strong **enhancement** at low invariant masses, which gradually **diminishes** at higher p_T .
- For v_2 and v_4 , distinct differences are observed at low invariant mass (around 0.1 GeV) compared to higher mass regions.

Needs a detailed study, currently work in progress.....



Scan for detailed information

Thank You!
Any Questions!

Numerical convergence

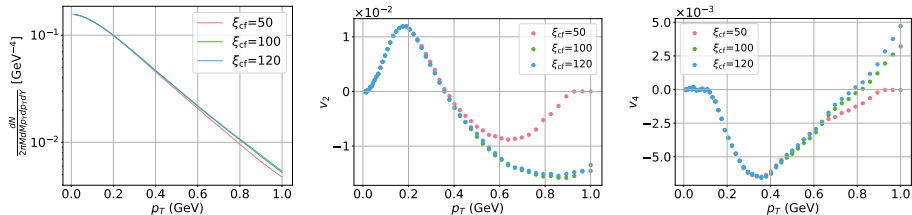


Figure: Numerical sensitivity of total spectra (left), v_2 (middle) and v_4 (right) for $b = 8$ fm, $\sigma = 5.8$ MeV and $M = 100$ MeV for three different choices of cutoffs $\xi_{cf} = 50, 100, 120$ respectively.

Magnetic field evolution

